American Journal of Engineering and Applied Sciences

Original Research Paper

Gas Atomization of Molten Metal: Part I. Numerical Modeling Conception

[1]Genaro Pérez-de León, [2]Vincent E. Lamberti, [2]Roland D. Seals, [1]Taher M. Abu-Lebdeh and [1]Sameer A. Hamoush

[1]Department of Civil, Architectural and Environmental Engineering, North Carolina A&T State University, Greensboro, NC, USA
[2]Oak Ridge Y-12 National Security Complex, Engineering Development Division, Oak Ridge-Tennessee, USA

Article history
Received: 07-04-2016
Revised: 08-04-2016
Accepted: 09-04-2016

Corresponding Author:
Taher M. Abu-Lebdeh
Department of Civil, Architectural and Environmental Engineering, North Carolina A&T State University, Greensboro, NC, USA
Email: taher@ncat.edu

Abstract: This numerical analysis study entails creating and assessing a model that is capable of simulating molten metal droplets and the production of metal powder during the Gas Atomization (GA) method. The essential goal of this research aims to gather more information on simulating the process of creating metal powder. The model structure and perspective was built through the application of governing equations and aspects that utilized factors such as gas dynamics, droplet dynamics, energy balance, heat transfer, fluid mechanics and thermodynamics that were proposed from previous studies. The model is very simple and can be broken down into having a set of inputs to produce outputs. The inputs are the processing parameters such as the initial temperature of the metal alloy, the gas pressure and the size of the droplets. Additional inputs include the selection of the metal alloy and the atomization gas and factoring in their properties. The outputs can be designated by the velocity and thermal profiles of the droplet and gas. These profiles illustrate the speed of both as well as the rate of temperature change or cooling rate of the droplets. The main focus is the temperature change and finding the right parameters to ensure that the metal powder is efficiently produced. Once the model was conceptualized and finalized, it was employed to verify the results of other previous studies.

Keywords: Gas Atomization, Molten Metal, Metal Powder, Heat Transfer, Droplet Dynamics

Introduction

As society increases, the demand for better utilization of our resources also increases. One new method that is currently being developed through research is production of molten metal droplets that can later be used in several applications such as Additive Manufacturing (AM), rapid prototyping, 3D printing, brazing and plasma/thermal spray. Several metals such as Aluminum (Al), Copper (Cu), Iron (Fe), Magnesium (Mg), Titanium (Ti) and Nickel (Ni) as well as alloys, when in powder form can have several applications (view Fig. 1). They can be used within the aerospace, automotive, biomedical and chemical industries to create a variety of objects. Additionally, 3D printing can utilize metal powder as micro-particles, which then can be implemented in several industries because they can make metals stronger and harder as well as augmenting ceramics to increase ductility and formability. Micro-particles can also enable normally insulated materials to conduct heat or electricity as well as produce protective coatings transparently (Giri *et al*., 2004). These metals or alloys can become a powder form through the various techniques of melt atomization within the powder metallurgy process field. Some of these techniques include Gas Atomization (GA) and Impulse Atomization (IA), with GA being considered a better option due to the amount of control for desired results through the selection of powder chemistry, gas composition and powder size distribution. A brief description of GA can be defined as when molten metal is disrupted or disintegrated by a high or powerful velocity of gas.

Classifying each GA process is indicated by the velocity of gas jets as well as other factors. Once the pressure of gas is released from the chamber (high pressure to low pressure), it makes contact with the molten metal liquid at high velocity. The liquid then becomes spherical droplets due to the impingement. Further details and information in regards to GA can be found in the subsequent sections, but an example of a gas atomizer can be seen in Fig. 2.

The goal of this study was to utilize previous studies and build a complete, useable and simplified model that is able to simulate the production of a molten metal or alloy droplets based on a given set of properties and equations. The model utilizes heat transfer, fluid mechanics and thermodynamics to implement the simulation, while also applying energy balance, gas dynamics and droplet dynamics between the atomizing gas and droplets that are created from the melt stream. After the model is completed, previous studies were utilized to verify the accuracy and precision of the model as well as its capabilities using the governing equations and assumptions. Zheng *et al*. (2009a) were able to study the thermal history and cooling rates that occur for gas-atomized Aluminum (Al)-based amorphous powders through numerical simulations. The product of powder from gas atomization can be used in metallurgical techniques to create engineering metallic glass (MG) components. The other study carried out by Zheng *et al*. (2009b) was utilized to verify the data simulated from part I. It consists of using two materials, commercial Al 2024 and metallic glass (MG) Al90Gd7Ni2Fe1. They were able to validate a good agreement between experiment (part II) and numerical simulation (part I) results. Also noted, was that by completing a numerical framework study that provided details, they were able to limit the amount of experimentation required.

Fig. 1. Different metals in powder form (EFMPCL., 2008)

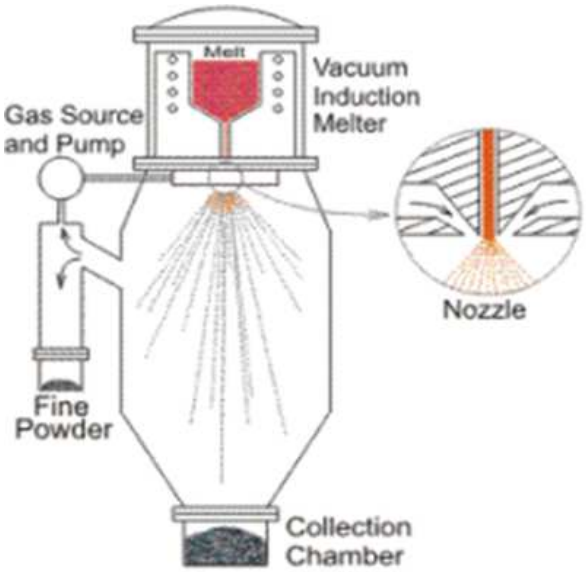

Fig. 2. Design of vertical gas atomizer (AMT, 2014)

Modeling Program

Methodology

The actions necessary to complete this numerical analysis study first started with knowing the proper equations and assumptions before creating the model. Equations and assumptions correspond with those observed in the research conducted by Zheng *et al*. (2009a) for the studies in both parts. Modeling the droplet and particle creation heavily relied on mathematical and numerical analysis within MATLAB™. Two main solvers that were utilized to differentiate and find the necessary results were (ordinary differential equations) ode45 and ode15s. The first is a one-step solver that computes inputs based on an explicit Runge-Kutta formula (the Dormand-Prince pair) (Dormand and Prince, 1980). The latter is a multistep solver that computes in a variable order solver based on numerical differentiation formulas (Shampine and Reichelt, 1997). In addition, ode15s is able to use the backward differentiation formulas (also known as Gear's method) and is useful when ode45 fails or is not efficient. (Shampine and Reichelt, 1999)

As previously mentioned, the assumptions listed below correspond with those obtained from previous studies and were implemented:

- Spherical droplets were created at gas impingement point, which is where the droplet velocity and flight distance is zero
- Modeling was based on Newtonian cooling (homogenous temperature inside of a droplet) with forced external convection
- No nucleation occurring before the droplet temperature reaches the glass transition temperature when the material is an alloy
- Droplets travelled along chamber axis and were subject to same gas velocity profiles, no matter the size
- Considerations of radial distance were not taken into consideration, solely axial distance was accounted for in regards to flight distance
- During the solidification of the droplets, several factors were ignored, these factors are as follows: The phase transformation, crystal nucleation and growth (as a substitute, energy conservation or balance was utilized)
- Through the application of specific heat capacity as a function of temperature, the difference of the specific heat between liquid and solid is not taken into consideration
- Droplet density remains constant and fluctuations in local gas velocities caused by turbulence were ignored; only the mean gas flow was considered

Equations

Following Zheng *et al*. (2009a), the following equations were implemented within the model.

Gas Dynamics

Gas initial velocity follows the laws of fluid mechanics and applies the necessary concepts:

$$v_{g0} = M_a * v_s \tag{1}$$

The application of a convergent–divergent atomizer in the model falls under compressible fluid mechanics and entails steady state and isentropic flow for an ideal gas. This concept is used to find Mach number (refer to Equation 2):

$$M_a = C_M * \left[\frac{2}{\gamma - 1} * \left[\left(\frac{P_0}{P_e} \right)^{\frac{\gamma - 1}{\gamma}} - 1 \right] \right]^{\frac{1}{2}} \tag{2}$$

$$v_s = \left(\frac{\gamma * R * T_e}{m_{mol}} \right)^{\frac{1}{2}} \tag{3}$$

$$\frac{T_0}{T_e} = 1 + \frac{\gamma - 1}{2} * M_a^2 \tag{4}$$

Following the notion that axial gas velocity decays exponentially with axial flight distance, the axial gas velocity can be found (refer to Equation 5) (Grant, 1995):

$$v_g = v_{g0} * \exp^{\left(-\frac{z}{\lambda}\right)} \tag{5}$$

$$\lambda = 3.04 * 10^{-4} * v_{g0}^{1.24} \tag{6}$$

Droplet Dynamics

Each droplet within the GA process is accelerated or decelerated due to drag force, which is a product from the velocity difference with the local atomization gas. Motion of the droplet occurs along the spray-axis (refer to Equation 7):

$$\begin{aligned} &\rho_d V_d \left(\frac{dv_d}{dt} \right) = V_d \left(\rho_d - \rho_g \right) g \\ &-\left(\frac{1}{2} \right) \rho_g A_s C_d \left| v_d - v_g \right| \left(v_d - v_g \right) \end{aligned} \tag{7}$$

where, $V_d = \frac{\pi}{6} * d^3$ and $A_s = \frac{\pi}{4} * d^2$.

$$C_d = 0.28 + \frac{6 * \sqrt{\mathrm{Re}} + 21}{\mathrm{Re}} \tag{8}$$

$$\mathrm{Re} = \frac{\rho_g * d * \left| v_g - v_d \right|}{\mu_g} \tag{9}$$

Energy Balance Equations

A temperature difference amid the droplets and gas is large. The droplets are in a state of molten metal and the gas is pressurized. Throughout the flight of the droplet, heat extraction occurs from the droplet by means radiative and convective cooling. From the spectrum of different sized droplets and processing parameters, heat conduction within the droplets can be ignored. Also, for this model, homogenous temperature distribution inside the droplets is assumed to fall under Newtonian cooling conditions. Forced convection also occurs in the process because of the Biot number magnitude. The magnitude of the Biot number (Bi) that ensures forced convection is due to the droplets relative to the droplet/gas interfacial heat transfer that is less than 0.1 and on the scale of 10^{-3} to 10^{-2}. When the Bi is less than 0.1, the temperature difference or thermal resistance across the inside of the droplet can be ignored. With the Bi also being so small, this essentially ensures that this portion of the model is thermally simple, due to the uniformity of temperature inside the droplets. Cooling of the droplet during the flight phase follows two sequential processes. The processes are liquid-phase cooling and solid-phase cooling. Using these concepts, the energy conservation can be found (refer to Equation 10). It is also important to note that due to the assumption of no phase transformation, the difference between liquid and solid specific heat is ignored when finding thermal profile values.

$$\begin{aligned} &-h * fr * A_d * \left(T - T_{gas}\right) - A_d * \varepsilon * \sigma * \left(T^4 - T_{gas}^4\right) \\ &= V_d * \rho_d * C_{pd} * \left(\frac{dT}{dt}\right) \end{aligned} \tag{10}$$

where, $\sigma = 5.671 * 10^{-8} \frac{W}{m^2 * K^4}$, $A_d = \pi * d^2$ and $C_{pd} = 21.8 + 0.009 * T$):

$$h = \frac{K_g}{d} * \left(2 + 0.6 * Re^{\frac{1}{2}} * \mathrm{Pr}^{\frac{1}{3}}\right) \tag{11}$$

$$\mathrm{Pr} = \frac{(\mu_g * C_{pg})}{K_g} \tag{12}$$

Droplet thermal behavior is affected by several parameters such as the gas composition, gas pressure, the gas/melt mass flow ratio, melt superheat temperature, droplet size and alloy composition. Furthermore, heat that is released by convection at a droplet's surface can be tantamount to the alteration of the droplet temperature (refer to Equation 13):

$$\dot{T} = \frac{6 * fr * \left(T_{melt} - T_{gas}\right) * h}{C_{pd} * d * \rho_m} \tag{13}$$

The consideration corresponds with a nozzle diameter of 2.16 mm. f_r is the gas/melt flow ratio.

Model Properties

The properties tabulated in Table 1 correspond with the properties of the selected gas and its composition, which can be mixture of Ar and He. Properties of the gas composition can be obtained through the use of volume percentages that make up the entire gas composition for Ar and He, respectively. The properties below in Table 2 correspond with the properties of the material (Al90Gd7Ni2Fe1) utilized in this model for conception and other important values. The same types of property values found below are also utilized when verifying the model.

Gas and Droplet Dynamics Application

Results that reflect the motion of the gas/droplet for this model was obtained by utilizing equations 1 through 10. Through the application of these equations the data was able to show the velocity profile of the droplet and gas at a certain droplet diameter size (20 μm) under different gas pressures as well as the velocity profile of the droplet at different droplet diameter sizes at one gas pressure (2.76 MPa). Flight time or time that the droplet falls during the process is utilized to illustrate the velocity variation of the droplet and gas under certain droplet diameter size under different gas pressures. Flight distance or distance that the droplet travels during the process is utilized to illustrate the velocity variation of the droplet at different droplet diameter sizes at one gas pressure.

Thermal Behavior of Droplets Application

The thermal behavior of the droplets can be assessed from the cooling rate that the droplets exhibit throughout the GA process. Equations 1 through 10 as well as equations 11 through 13 are used to show the droplet thermal behavior. These equations allowed the model to illustrate the droplet cooling rate during flight in GA at different droplet diameter sizes. The gas composition (He 100%) and gas pressure (2.76 MPa) remained constant. Equation 13 is able to show the cooling rate because it is based on the consideration of heat transfer and shows that the heat loss from the droplets is from forced convection. The forced convection is roughly two orders of magnitude larger than the loss by radiation and to ensure that the cooling rate can be observed, the radiation from Equation 10 is ignored.

Table 1. Physical and thermal properties of He and Ar (Zheng *et al*., 2009a)

Symbol	Values	Unit
m_{mol}, *Ar*	40	g/mol
m_{mol}, *He*	4	g/mol
m_{mol},*mixture*	m_{mol}, mixture = 40 x_{Ar} + 4 x_{He}	g/mol
μ_g, *Ar*	224.3	10^{-6} *Ns*/m^2
μ_g, *He*	198.6	10^{-6} *Ns*/m^2
K_g, *Ar*	0.0179	$\frac{W}{m*K}$
K_g, *He*	0.15015	$\frac{W}{m*K}$
C_{pg}, *Ar*	520.67	$\frac{J}{kg*K}$
C_{pg}, *He*	5278	$\frac{J}{kg*K}$
ρ_g, *Ar*	1.5979	kg/m^2
ρ_g, *He*	0.1624	kg/m^2

Table 2. Properties of alloy Al90Gd7Ni2Fe1 (Zheng *et al*., 2009a)

Symbol	Values	Unit
ρ_m	3545.0000	kg/m^2
C_M	0.2165	-
ε	0.0350	-
T_g	464.0000	*K*
T_m	916.0000	*K*
T_0	300.0000	*K*

Effect of Processing Parameters on Droplet Cooling Rate and Temperature Application

The sections below describe areas of influence that the processing parameters had on the velocity and thermal profiles of the gas and droplets used within the model.

Gas Composition

Gas composition can influence the droplet temperature and cooling rate. Equations 1 through 12 were utilized to show how the influence of gas composition on droplet temperature can cause variation at one selected droplet size. The gas composition ranges from 100% Ar to 100% He, with 20% increment sizes as one increases as the other decreases, while the droplet size remains the same. Furthermore, another aspect was the effect or influence of gas composition on the cooling rate while the droplet size changes, which utilized equations 1 through 13. The gas composition altered from 0 to 100% He in increments of 10%, while the amount of Ar decreased by 10%. Droplet diameter sizes were 5, 20 and 60 μm. This aspect illustrated cooling rate as a function of the He percentage in the gas composition, which was used in the GA process.

Gas Pressure

Furthermore, the pressure of gas can alter the cooling rate of the droplets within the GA process. Utilizing equations 1 through 13 allowed for data to demonstrate how different gas pressures can alter the droplet temperature at one droplet size as a function of flight time. Another area of focus is how much the cooling rate of the droplets can depend on increasing gas pressure within the process. Gas pressure begins roughly at 0.75 MPa and ends at roughly 10.21 MPa. These two areas can help decide how each can influence the cooling rate and droplet temperature as well as provide further insight on how each can possibly provide the proper optimal parameters.

Droplet Diameter Size

This data also shows how droplet temperature varies as the size of the droplet changes as a function of flight time. The gas composition and gas atomization pressure remain constant, as the droplet size changes. Droplet size though can vary greatly depending on the material selected for the study or the desired results for the process. Illustrating this point requires utilizing Equations 1 through 12.

Melt Superheat Temperature

The effect that melt or droplet superheat temperature has on droplet cooling rate is found in this section. Modeling this required that the atomization gas pressure (2.76 MPa), droplet diameter size (20 μm) and gas composition (100 He%) remained constant. Results from this section can provide insight on the powder size distribution and other factors. In order to get results, equations 1 through 13 were utilized.

Influence of He Versus Gas/Melt Flow Ratio

The last aspect of the effect of processing parameters on droplet cooling rate and temperature entails observing the variation of cooling rate on two sets of parameters. One aspect focuses on how the cooling rate can change

as a function of the droplet diameter size and the other focuses on how the cooling rate changes as a function of flight time, for the two different parameters. The two sets have the same gas pressure and initial melt superheat temperature, but both have different gas compositions to account for the change in nozzle orifice diameter as well as gas/melt flow ratio.

Results

Conception

The sections below correspond with the methodology and results obtained from assembling as well as executing the model within MATLAB™. The following figures represent the results of the numerical modeling of Al alloy (Al90Gd7Ni2Fe1) and an atomization gas (He-Ar mixture). Additionally, this section served as a key component in building the model for later use in obtaining new results for different alloys.

Gas and Droplet Dynamics

In the figures below, the objective was to gain a better understanding of how the velocity of the gas and droplet can be affected through the use of different processing parameters. Figure 3 demonstrates that gas pressure can have a significant influence on both gas and droplet velocity with respect to flight time. There is a direct correlation showing that as the atomization gas pressure increases both the gas and droplet velocity. The droplet velocity increases because of the effect of the gas velocity when it creates contact with the droplet after the dispersion of the melt stream, which creates droplets. The droplets undergo initial acceleration, but once gas velocity is surpassed, the droplet velocity decreases because of the impeding drag force from the gas. Viewing the figures show this behavior at the intersection of the gas and droplet velocities or lines, both velocities gradually decrease as the flight distance increases. Gas velocity reaches its maximum at the exit of the atomizer nozzle and decreases with uniformity. In order to produce comparable and consistent results, the droplet diameter size was held constant at 20 µm.

Figure 4 illustrates what happens when the gas pressure is held constant, while the droplet diameter sizes increase from 5 to 60 µm. It is evident from these figures that even though the gas pressure remains constant, the droplet velocity decreases as the droplet diameter size increases. For droplet diameter sizes from 5 to 20 µm, the droplets still portray a form of exponential decrease, however at 40 to 60 µm; the droplets do not portray that behavior. This happens because as the droplet diameter size increases, so does the inertia and size, which causes a less amount of change in the velocity because of the larger droplets ability to repel the acceleration force. These figures plotted velocity of gas and droplets with respect to flight or axial distance (radial distance not considered).

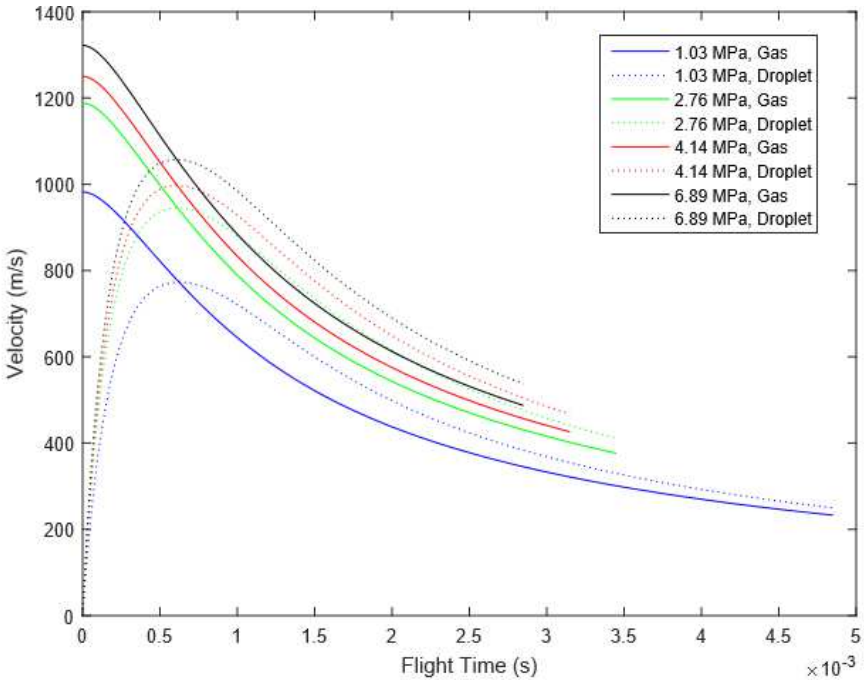

Fig. 3. Velocity profile of gas and droplets at 20 µm under different gas pressures

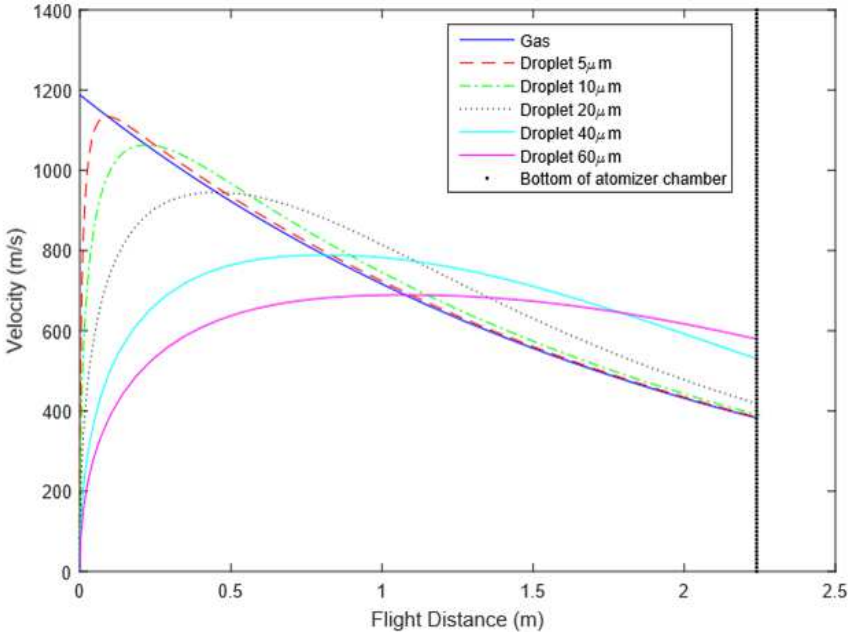

Fig. 4. Velocity profile of atomization gas and droplets at a gas pressure of 2.76 MPa

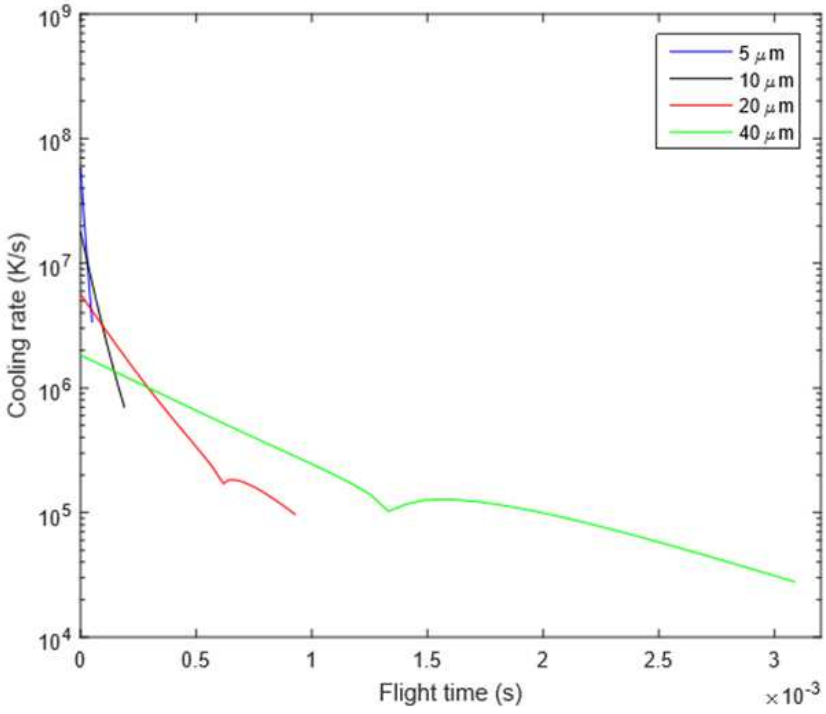

Fig. 5. Cooling rate at different droplet diameter sizes during GA process

Thermal Behavior of Droplets

The Fig. 5 demonstrates the cooling rate of droplets from sizes of 5 to 40 μm, with respect to flight time. Cooling rate was obtained by considering the melt superheat temperature, gas temperature, droplet diameter size, melt specific heat and the convective heat transfer coefficient. The convective heat transfer coefficient is derived from a Ranz-Marshall correlation, which considers the thermal conductivity of the gas, droplet diameter size, the Prandtl number and Reynolds number. Below it is hard to see the behavior of the smaller range

of droplets (5 to 10 μm), but the behavior of the larger droplets (20 to 40 μm) are visible. One clear depiction is that as the droplet diameter size increases, the cooling rate decreases. The equations to find cooling rate also indicate that a higher convective heat transfer coefficient produces higher cooling rates, because of the higher relative velocity (difference of gas and droplet velocity).

Effect of Processing Parameters on Droplet Cooling Rate and Temperature

Gas Composition

This section shows droplet temperature at an initial melt superheat temperature held constant and how gas composition can affect droplet temperature with respect to flight time. Furthermore, altering the gas composition from 100% Ar to 100% He, but keeping the droplet diameter size and gas pressure constant is illustrated with the Fig. 6. It is clearly evident that as the increase of He is used, the droplet temperature decreases rapidly. This is highly important, because this can lead to effective manufacturing processes to produce metal alloy powders at quicker rate, leading to rapid solidification. This feature is also shown in Fig. 7. Once again, gas composition plays a key role on the droplet cooling rate. These figures illustrate the cooling rate of the droplet with respect to He fraction. This is a better visualization that illustrates a correlation, that as the amount of He is increased within the gas composition, the cooling rate increases as well. Each line denotes a droplet diameter size held constant at one gas pressure and one melt superheat temperature. These figures also show that, having a smaller droplet size produces a higher cooling rate.

Gas Pressure

Figure 8 illustrates droplet temperature with respect to flight time. This figure held the droplet diameter size constant along with the gas composition at He-100%. However, gas atomization pressure was ranged from 1.21 to 10.34 MPa. It can be seen that gas atomization pressure does not strongly influence the droplet temperature, because the lines are in proximity to each other. It is also apparent that as the melt super heat temperature increases, the cooling rate increases as well. This is attributed to the change in temperature gradient amongst the gas and the melt stream.

Figure 9 shows the cooling rate with respect to gas atomization pressure. This figure is plotted with the y-axis at a set range in a logarithmic manner, while the droplet diameter size, melt superheat temperature and gas composition are held constant. Viewing this data, shows that once the gas atomization pressure reaches approximately 2.76 MPa and beyond, the cooling rate beings to flatten or remain constant. There is no significant change as opposed to when the gas atomization pressure is less than 2.76 MPa, because the cooling rate shows a rapid increase of change. Taking into consideration all the figures in this section, it is also indicative that gas atomization pressure has an effect on the cooling rate, but gas composition has a stronger influence on the cooling rate.

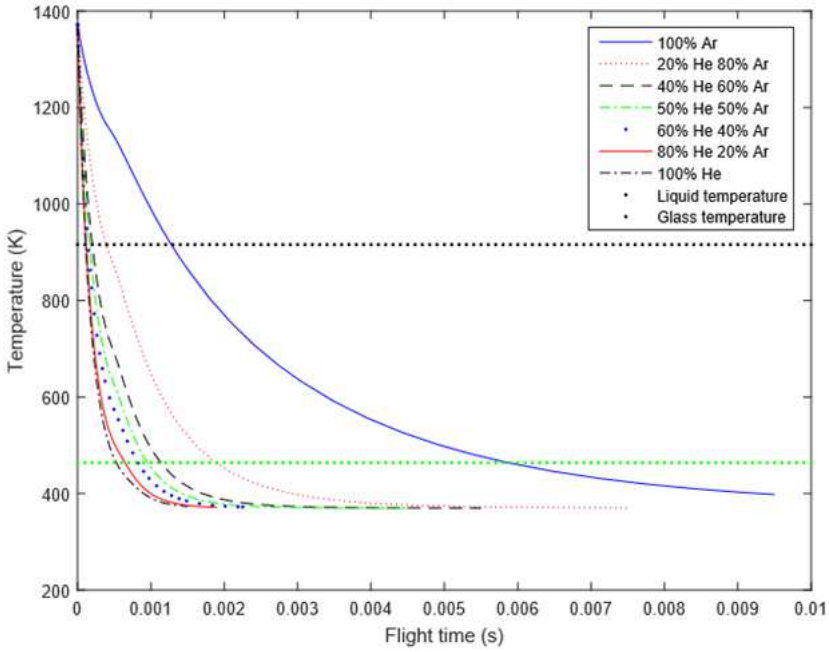

Fig. 6. Gas composition influence on temperature for 20 μm droplets at 2.76 MPa

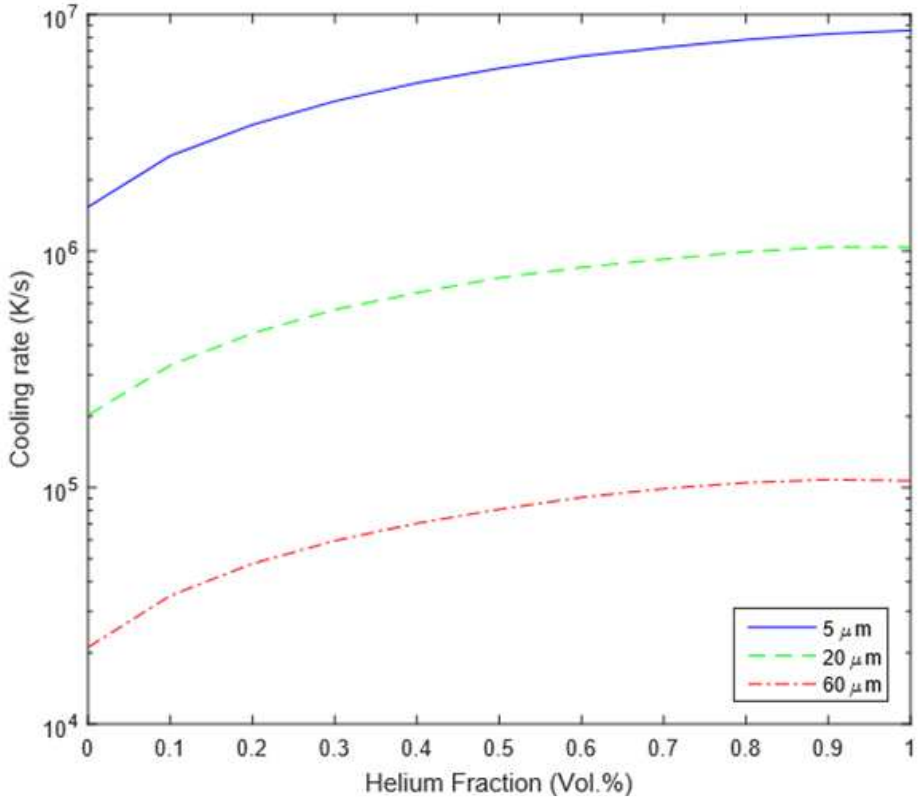

Fig. 7. Gas composition influence on droplet cooling rate at different sizes

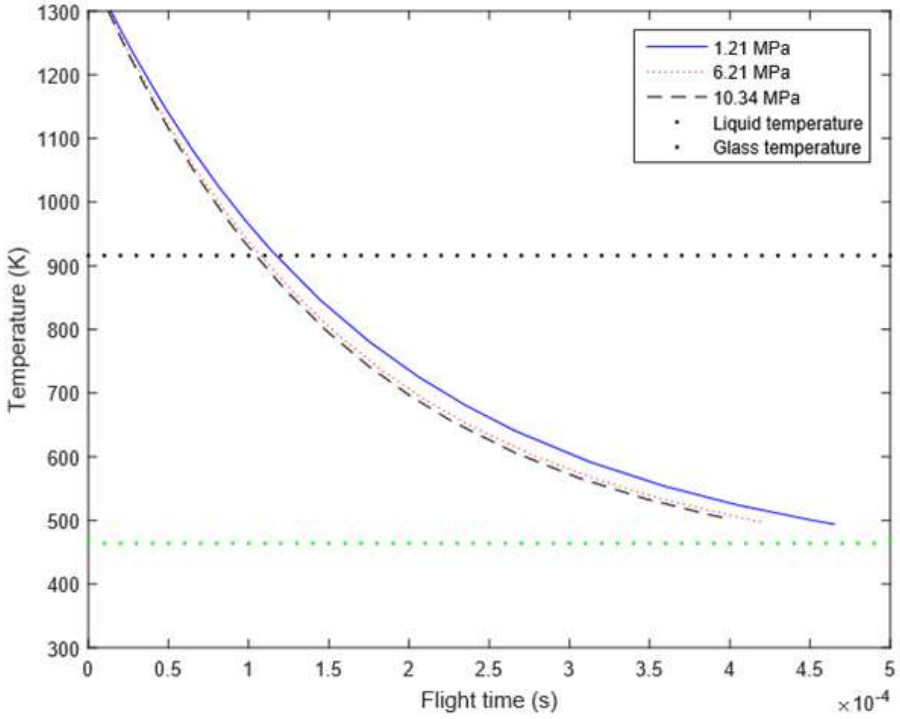

Fig. 8. Droplet temperature for 20 μm droplet from 1.21 to 10.34 MPa at 100% He

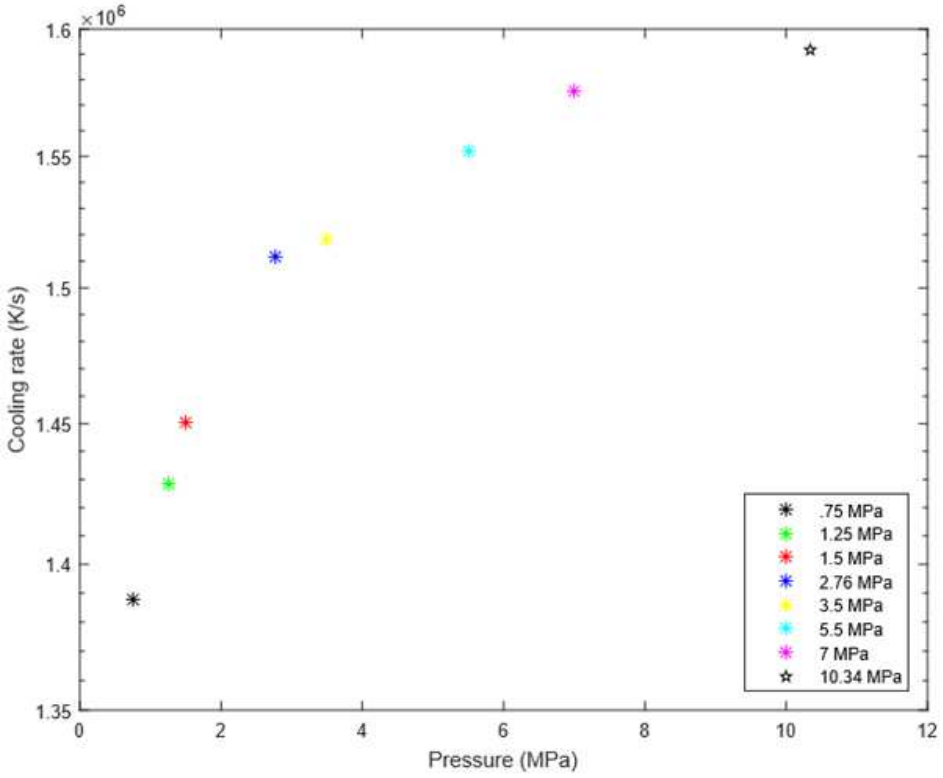

Fig. 9. Effect of gas pressure on cooling rate at 20 µm droplet diameter size

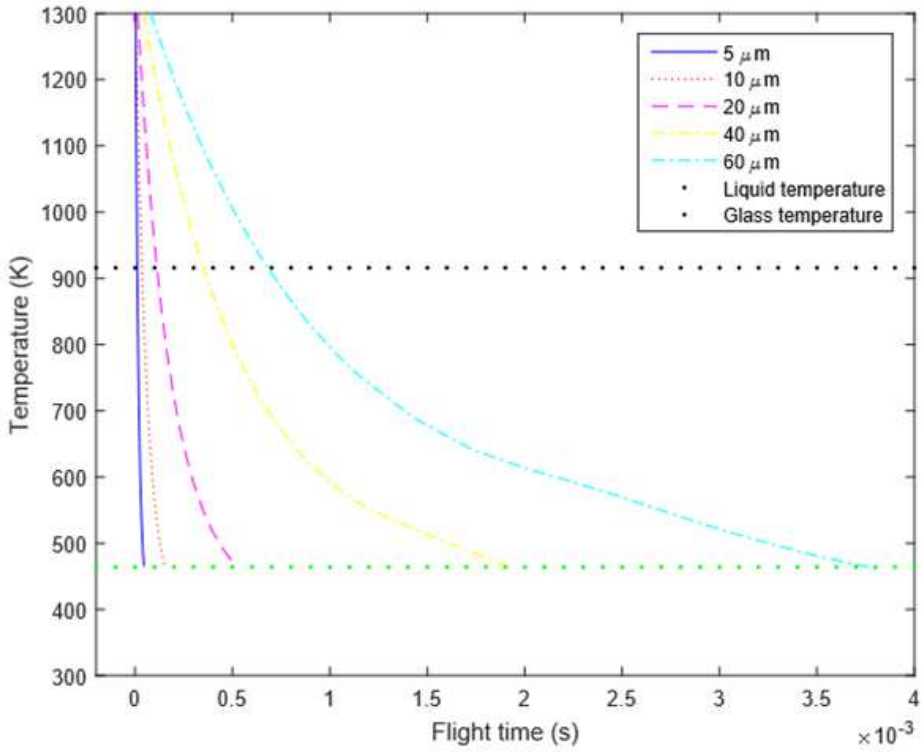

Fig. 10. Droplet temperature for 5 to 60 µm droplet(s) at 2.76 MPa and 100% He

Droplet Diameter Size

This section focuses on selecting which droplet diameter size to utilize in the simulation and numerical modeling of molten metal powder production. Figure10 is set to show droplet temperature with respect to flight time, by keeping the melt superheat temperature, gas atomization pressure and gas composition constant while changing the droplet size from 5 to 60 µm. It is indicative that when the droplet diameter size is below 20 µm, the droplets cool at a much faster rate and the size does not prove to be a strong influence on the droplet temperature. However, once the droplet diameter size is 40 µm and greater, the droplets take a longer time to cool and solidify. Results also suggest that selecting a droplet diameter size of 20 µm or less will produce a faster time of solidification.

Melt Superheat Temperature

This section concentrates on the effect of melt superheat temperature on cooling rate with respect to flight time. In order to produce the results in Fig. 11, the gas atomization pressure, gas composition and droplet diameter size were held constant, while the melt superheat temperature ranged from 1273 to 1473 K. It is clear that melt superheat temperature does not strongly influence the cooling rate for this material at these conditions. Figure 11 depicts how all lines are in proximity of each other and emulate a similar behavior of a gradual decrease. Additionally, as the melt superheat increases, the cooling rate increases as well.

Influence of He Versus Gas/Melt Flow Ratio

Figure 12 depicts the cooling rate in a logarithmic manner with respect to the droplet diameter size. The gas composition was altered while the atomization gas pressure, droplet diameter size and melt superheat temperature remained constant. Observing the figure demonstrates the effect of gas composition and nozzle orifice or opening size on cooling rate. These results suggest that by having a higher amount of He in the gas composition, the nozzle size can remain unaffected. One of the disadvantages or areas of concern with GA is that when the nozzle size is decreased or minimized to produce a thinner melt stream, the occurrence of premature cooling or solidification can occur. With the figures below, this occurrence can become mitigated through the use of a higher content of He in the gas composition. Next Fig. 13, depicts cooling rate in a logarithmic manner with respect to flight time. As previously mentioned, the gas composition was altered while the atomization gas pressure, droplet diameter size and melt superheat temperature remained constant. These figures produce results that suggest that the cooling rate by the higher content of He has a greater cooling rate than the one with a lower He content initially, but as the GA process continues, the higher content He ends up cooling the droplets at a faster rate than compared to the one with a lower He content in the same amount of time allotted. This further solidifies that a higher He content is more likely to produce fulfilling results.

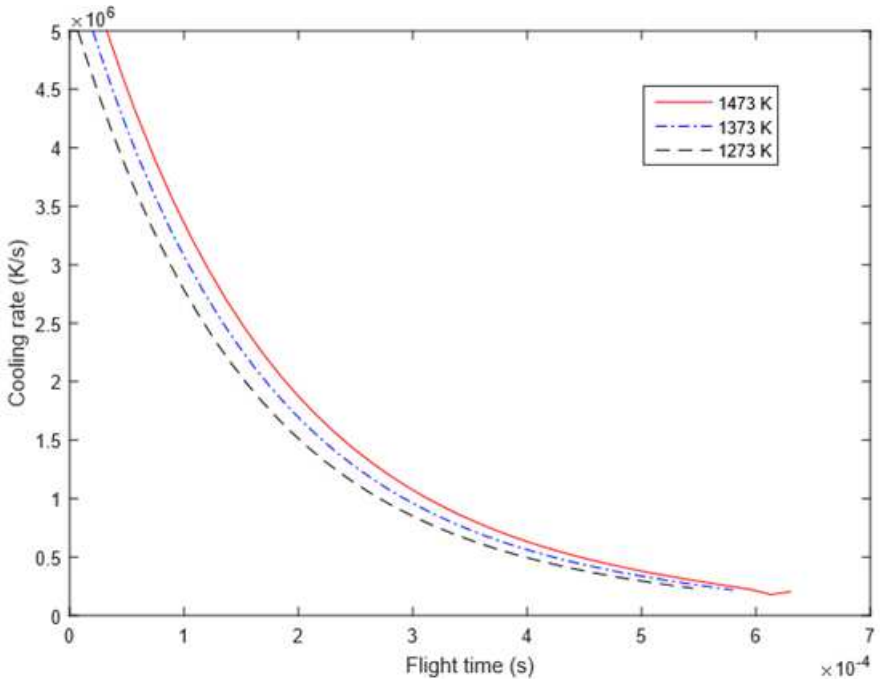

Fig. 11. Effect of melt/droplet superheat temperature on droplet cooling rate

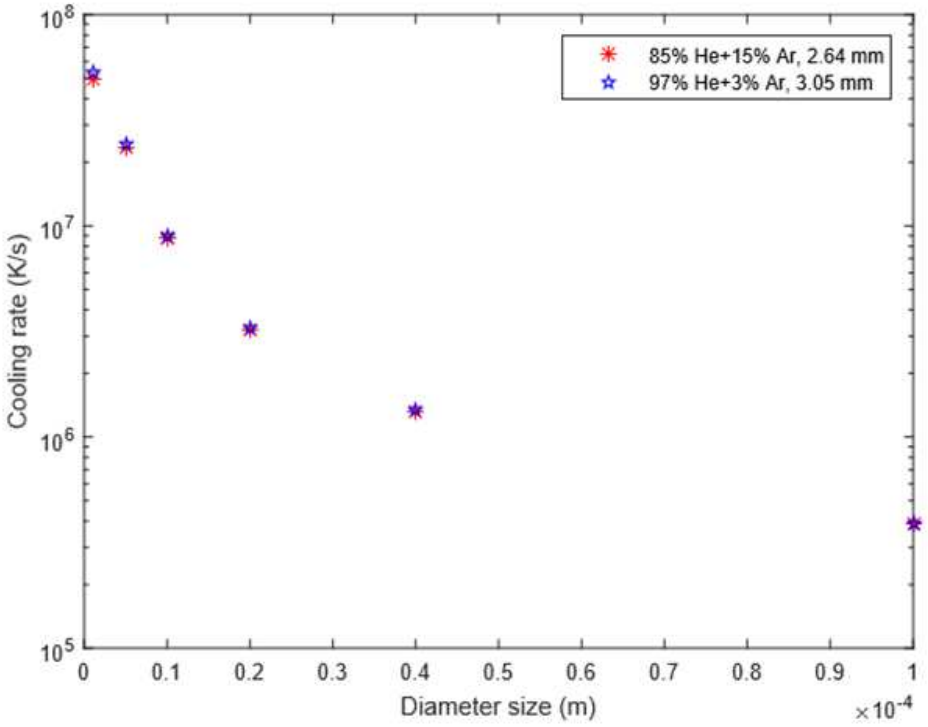

Fig. 12. Cooling rate for two sets of parameters as function of droplet size

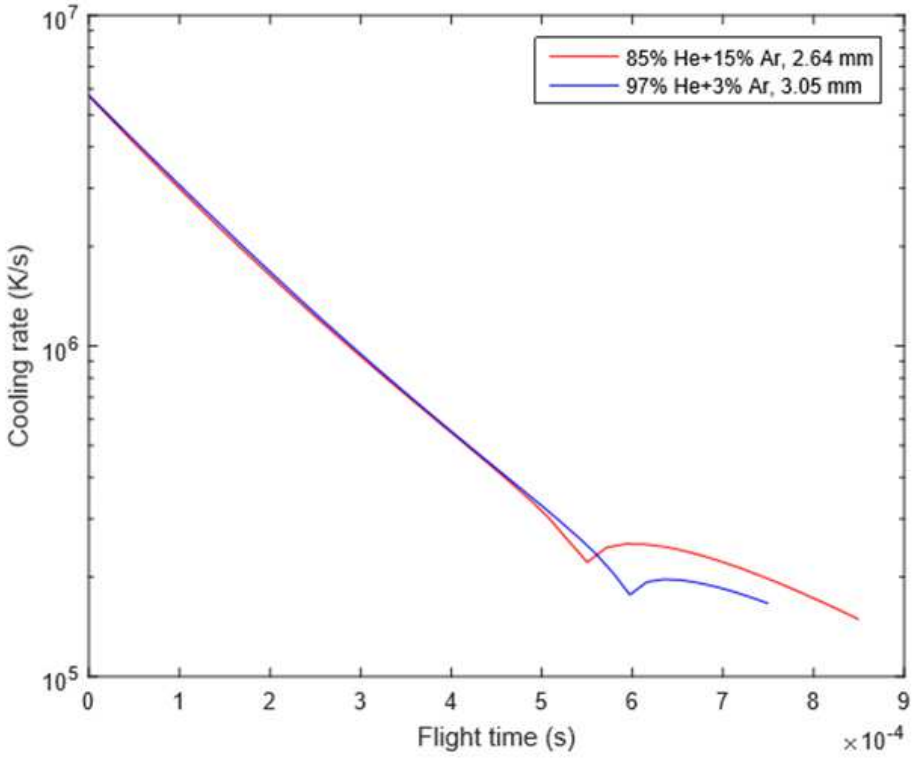

Fig.13. Cooling rate for two sets of parameters as function of flight time

Verification (First Study)

First study that was verified by this completed model was a study that utilized a metal alloy known as gamma-Titanium Aluminide (γ-TiAl), which is a light-weight, good ignition resistance and innovative alloy. In that composite, Ti is roughly 52% of the make-up and Al is at roughly 48%. Some applications of this alloy include being implemented in aerospace and automotive applications (Clemens and Smarsly, 2011). This model assumed the droplet motion consisted of two-Dimensional (2D) travel, which means the droplet is traveling axially and radially. Radial is in the latitude distance, while axial is the longitude distance. Fraction solidified is also considered and some governing equations are similar, but there are some differences within used factors. For example one notable difference is the manner of which the drag coefficient (which impacts the gas and droplet velocity profiles), droplet temperature as well as cooling rate are found, in regards to equations utilized. Another assumption that can also have an effect on their results versus this model is that study took temperature parameters such as initial, nucleation, liquidus and peritectic into consideration. Additionally, the atomization gas selected for use in this study was pure Ar. The objective was to gain more clarity on the momentum and thermal behavior of the metal during spray atomization and deposition. Solely the processing parameters, atomization gas as well as metal properties were utilized to verify the results; the governing equations were not altered (Li *et al*., 1996).

Initially when verifying this model to this past study, the velocity profile of the gas and different sized droplets were found. As previously mentioned, the atomization gas was Ar-100% and the droplets ranged in size from 20 μm to 500 μm. The results from this verification velocity profile are consistent with the results found from the built model. Viewing Fig. 14 and 15, it is evident that a smaller droplet (fine) is more inclined to have a higher velocity than a larger (coarse) one due to the greater amount of force that is acted upon it. Once velocity profile was verified, the model was then utilized to produce figures for two different sized droplets.

Viewing figures of 29 and 30 display the results obtained from this model versus what the study was able to find. The droplets selected for comparison were of a fine and coarse size. The fine droplet was 20 μm and the coarse was 325 μm, both droplets were treated with a superheat melt temperature of 1885K. Results show that for the 20 μm initially the model deviates from the study values, but as the distance increases, the model and study results were similar. This deviation is due to the difference of assumptions and equations that were different for the model compared to the study. The results for 325 μm proved to be far better with slight deviations, but ultimately very similar. As noted earlier, as the droplet size increases, the cooling rate decreases. For example, viewing the Fig. 16 and 17 in comparison of each other illustrates that the smaller droplet reaches a lower temperature much faster as opposed to when the droplet is larger. This is consistent with the governing equations of energy conversation that demonstrates that a larger droplet takes a longer amount of time to cool and solidify, due to the increase of area and volume.

Second Study

Final verification consisted of utilizing a study that sought to apply particle packing theory, fluid mechanics, as well as particle thermal and dynamic behavior to model the porosity during spray forming of an alloy that consisted of Al and Cu (Al-4Cu). Some of the factors and parameters utilized consisted of porosity coefficient, particle packing density and sticking efficiency. The objective was to find the optimal parameters that could ensure low porosity. Those parameters though were not accounted for in this present model, therefore they are ignored. This study consisted of two parts, but the verification results were obtained from part I of the study and focus on the velocity and thermal profile of the Al-4Cu droplets (Cai and Lavernia, 1998a). One assumption of this two part study was that the droplets were classified into two groups: Fully liquid and completely solidified. Another assumption stated that the deposited droplets formed through a two-stage mechanism. First stage consists of the droplets making contact with the substrate and forming a random, dense mold and the second stage consists of the remaining droplets from the melt stream making contact with the mold and solidifying within the openings of the mold. Even though this model also uses an Al alloy, which means similar physical properties as the one used to build the current model, there are several differences in the manner of which data was found. These differences are the equations utilized such as the drag coefficient of droplet dynamics as well as other additional ones. Cai and Lavernia (1998b). Following the same process as the last verification study, the results and figures below illustrate the velocity and thermal profiles of the Al-4Cu alloy. Droplets ranged from 10 to 100 μm. The model was successful in producing similar results to what the study produced as well, despite the difference of assumptions and equations. Other proven facts were also validated as well by viewing the figures below. Figures 18 and 19 coincide with the previous velocity profiles, which show that as droplet size increases, the velocity decreases and the larger droplets do not undergo as much deceleration as the smaller ones. Figures 20 and 21 also coincide with previous completed thermal profiles and show that larger droplets exhibit a longer time to cool than their smaller counterparts. The smaller droplets within the same range of distance are able to drop their temperature at a

significant rate as compared to larger ones. It is also worthy to note the difference between the model and study results. As the droplet size increases the accuracy of the model decreases, this is apparent due to the difference of equations utilized such as the drag coefficient, which attributes to a greater difference of relative velocity calculations between the model and study. For example, the larger diameter causes a larger difference of Reynolds number and therefore a larger difference of velocity calculations among the two.

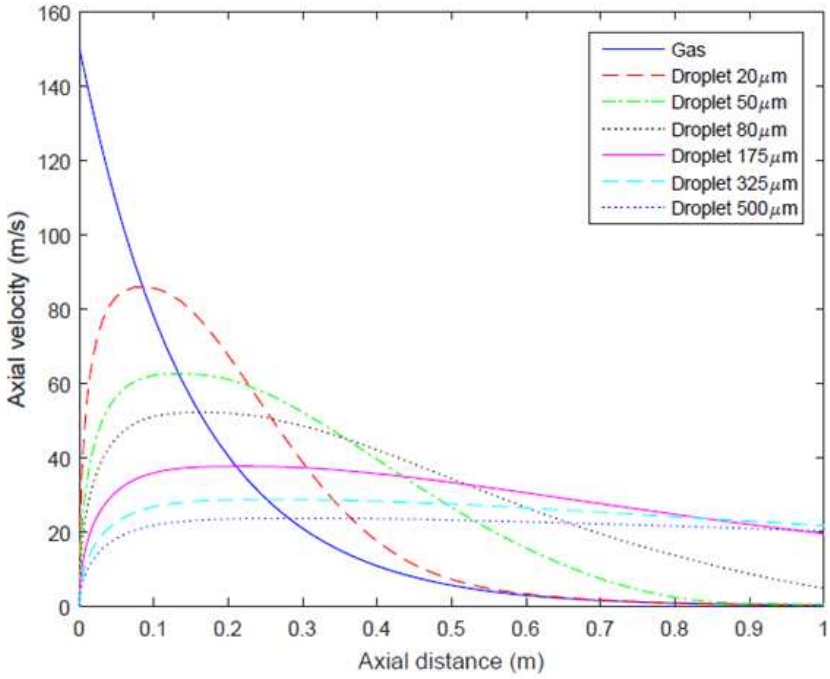

Fig. 14. Axial velocity profile of gas and droplets

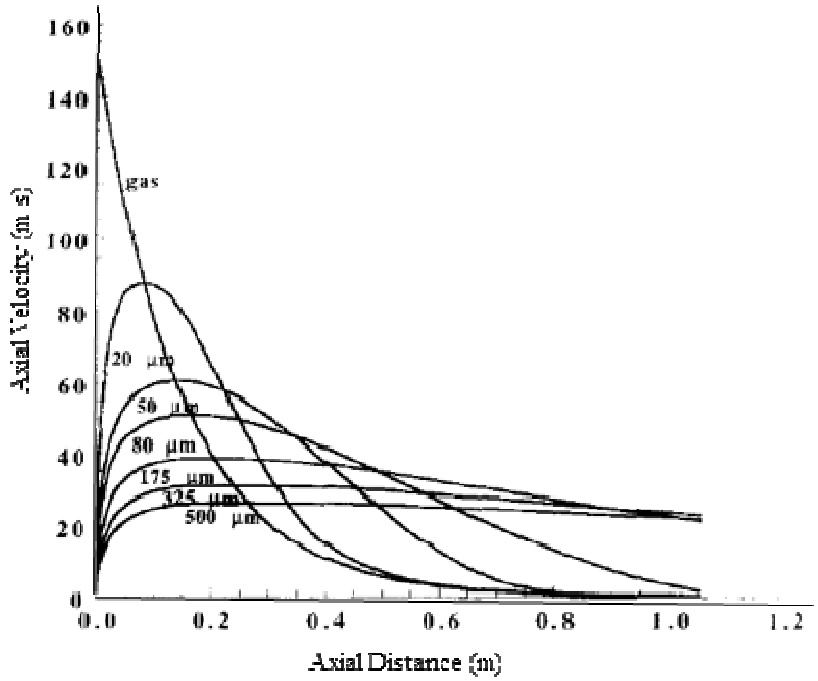

Fig. 15. Axial gas velocity and droplet velocities of γ-TiAl (Li *et al*., 1996)

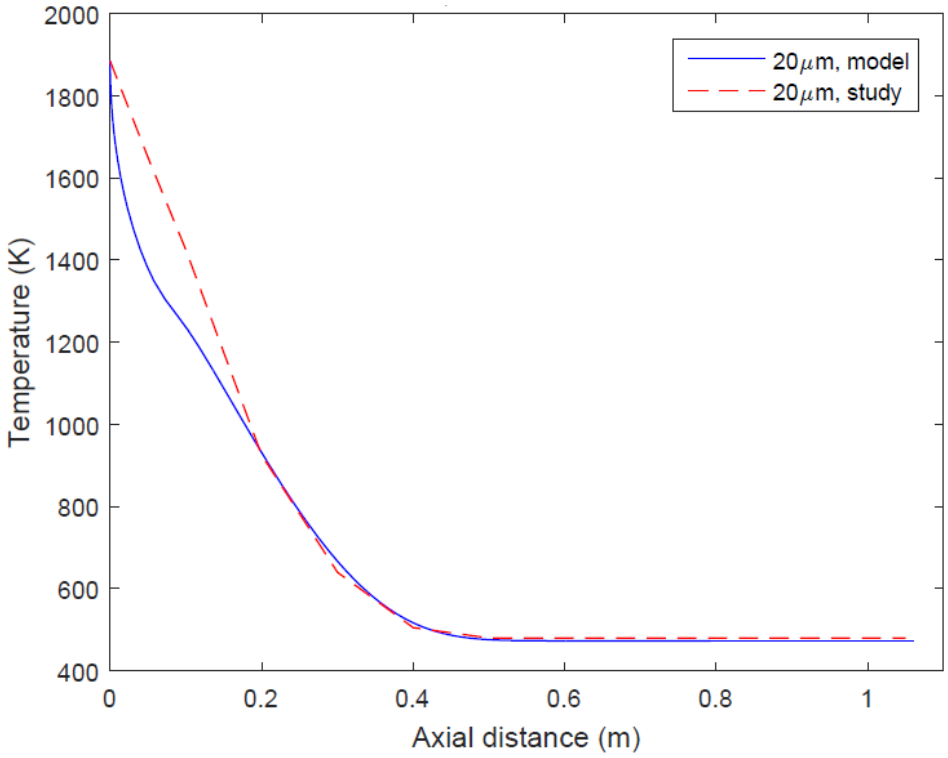

Fig. 16. Thermal profile of 20 μm droplet versus axial distance

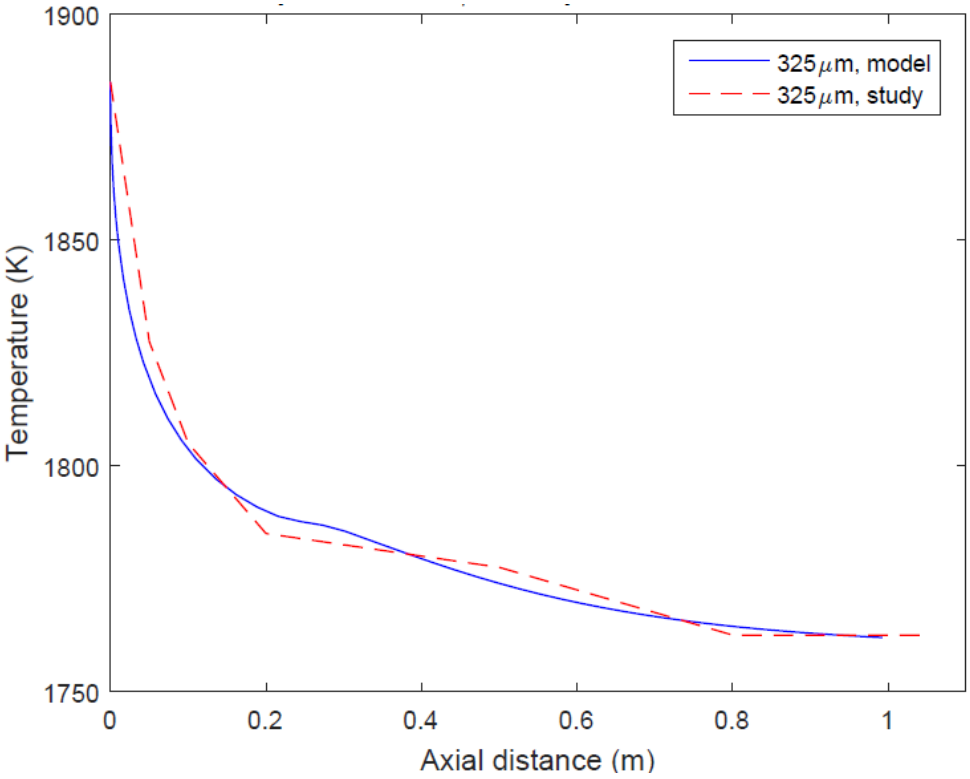

Fig. 17. Thermal profile of 325 μm droplet versus axial distance

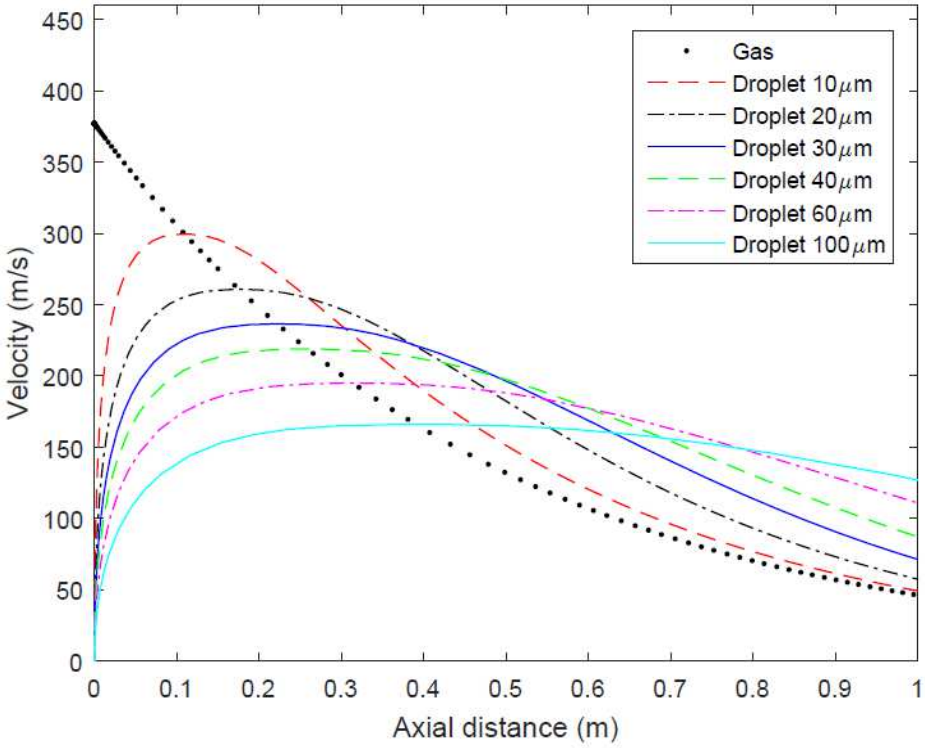

Fig. 18. Velocity profile of alloy (Al-4Cu)

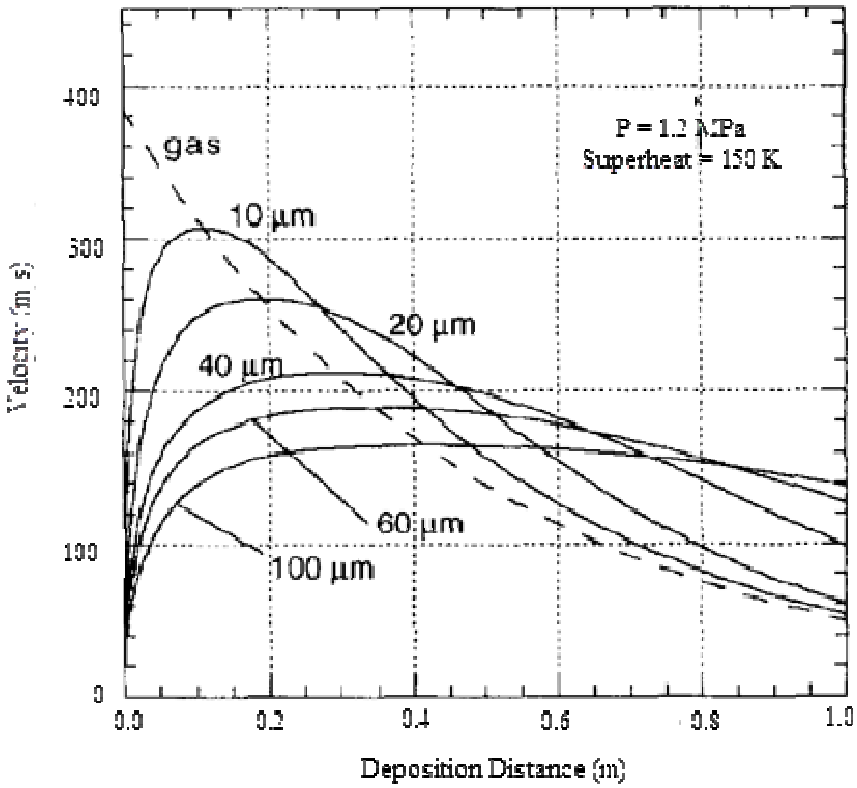

Fig. 19. Calculated gas and droplet velocities (Cai and Lavernia, 1998a)

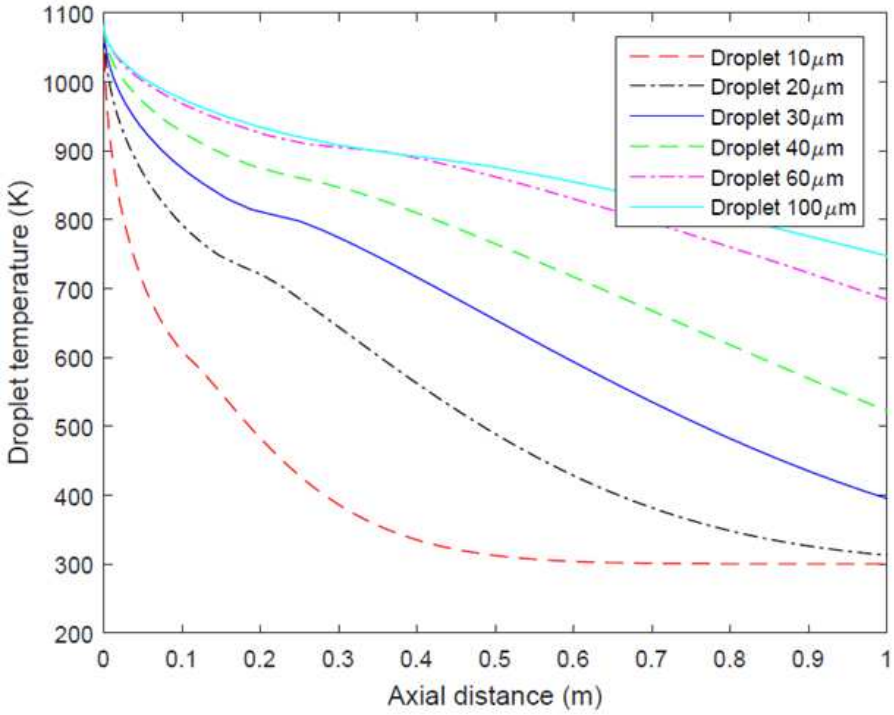

Fig. 20. Thermal profile of alloy (Al-4Cu)

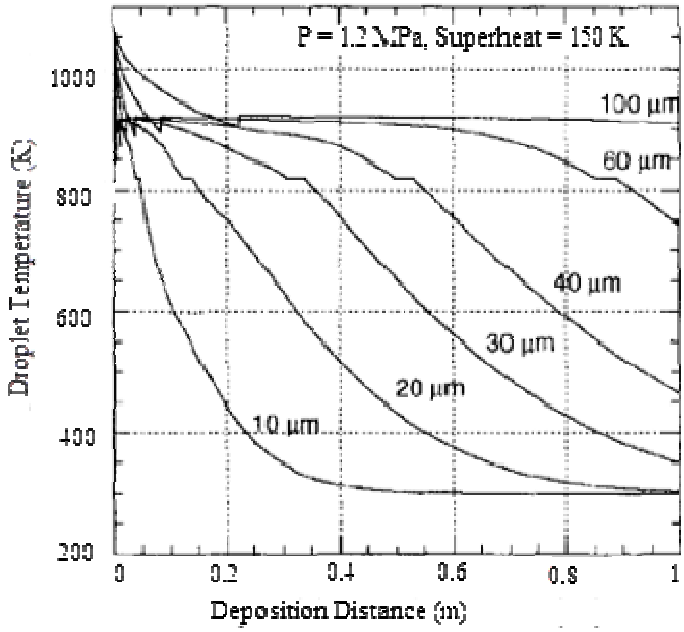

Fig. 21. Calculated droplet temperatures (Cai and Lavernia, 1998a)

Discussion

Parameter Selection

In regards to selecting the parameter selection, the two key parameters are the gas composition and droplet diameter size. Viewing the results in its entirety, it is evident that these two parameters play a significant role in producing molten metal powder. The results were able to simulate that other factors such as atomization gas pressure, melt superheat temperature and nozzle orifice

or opening size can influence the thermal profile, but they do not have a stronger influence than the gas composition and droplet diameter size. The Gas Atomization (GA) technique can essentially be defined as producing molten metal powder through the selection of the atomization gas and metal alloy. Previous stimulation studies have different assumptions in order to obtain results. This model however is simplified to render the results observable and manageable. Capabilities of this model include the ability to apply governing equations and aspects of fluid mechanics, thermodynamics and heat transfer to produce results that lead to a velocity and thermal profile. The governing equations utilized to find the velocity and thermal profiles are as follows: Gas initial velocity at the nozzle exit, Mach number at the nozzle exit, sonic velocity at the nozzle exit, ratio of temperatures, axial gas velocity, gas velocity decay coefficient, droplet motion along spray axis, spherical droplet during gas atomization drag coefficient, Reynolds number, droplet energy conservation, convective heat transfer coefficient (based on Ranz-Marshall correlation), Prandtl number and cooling rate of the droplets. Combing these equations fashioned results that illustrated all the different influences that can occur on the droplet temperature and cooling rate with respect to flight time, flight or axial distance, atomization gas pressure, droplet diameter size and He percentage of gas composition. Several of these figures proved that there are plenty of processing parameters to alter, but the main two to alter are gas composition and droplet diameter size selection. The reasoning behind this notion is further discussed below.

Gas Composition

As previously mentioned, gas composition can greatly affect droplet temperature and cooling rate far more superior as opposed to other processing parameters, such as atomization gas pressure and melt superheat temperature. Additionally, based on the results obtained, He proves to be a better selection as the atomization gas than Ar.It is worthy to note several property differences between He and Ar, which were utilized within this model. The molar mass and density for Ar is greater than that of He. Likewise, the thermal conductivity and gas specific heat of He is greater than that of Ar, while the dynamic viscosity for both are very similar to each other. These property differences prove that given the equations and results He is a more suitable atomization gas to utilize versus Ar. With He having a greater amount of values of thermal conductivity and specific heat capacity, it is able to garnish a greater efficiency in transferring heat. He absorbs the heat quicker and therefore, cools the droplets at a faster rate that than compared to Ar.

Droplet Diameter Size

Selection of the droplet diameter size also can have a strong influence on the results as well. This occurs from the increase of the droplet cross-sectional area, surface area and volume, through the increase of the droplet diameter size. The larger or coarse sized droplet has a greater area and volume, therefore is able to resist the acceleration and deceleration drag forces that are imposed on the droplets during GA, when compared to smaller or fine droplets. Having this greater size produces a lower velocity value which translates to lower cooling rates and change in temperature.

Results show that a larger droplet increases the amount of time the droplet can solidify, due to the larger volume and area. As the droplet size increases, the cooling rate decreases and the droplet takes a longer amount of time to coo. Smaller droplets cool faster because the heat within them is much less than that of a larger droplet. These larger droplets take a longer amount of time for the heat to leave them and transfer to the atomization gas; hence, smaller droplets produce greater values of cooling rate and are better suited as opposed to larger ones.

Verification of Model

In regards to verifying this current model to previous studies, it is proven that the model was successful. The first study consisted of verifying a γ-TiAl alloy with Ar employed as the atomization gas. The second study consisted of verifying an Al-4Cu alloy with N2 being the atomization gas. Some of the different assumptions from each study include; 2D modeling, which correlates to the droplet traveling in the radial and axial distance. This assumption was not taken into consideration for this model, as all distance for the droplets was taken into consideration as travelling axially. When comparing the studies selected for verification, it is notable that assuming 2D travel as opposed to 1D travel may be unnecessary when simulating the GA process and production of metal powder. Through visual inspection of model and study figures, it is apparent that despite the different assumption of 1D versus 2D travel, this model was still able to produce highly comparable results. This provides reasoning that solely the focus of droplet travel should be placed on axial travel and not radial.

Supplementary assumptions took temperature parameters such as initial, nucleation, liquidus and peritectic into consideration, while this model employed a specific heat capacity equation as a function of temperature to model those parameters and an energy balance or conservation equation was utilized. Another difference was how relative velocity was calculated in regards to taking the drag coefficient into consideration. Each study utilized a different set of equations than the

one from this model, but the model was still able to produce accurate and comparable results.

Conclusion

Gas atomization has become a popular form of melt atomization within the powder metallurgy community due to its abilities. It encompasses the utilization of an organized environment to forcefully cause the disruption of a melt stream that is composed of a selected metal alloy. The use of an atomization gas produces a quantity of metal powder that can later have applications in several industries. To concentrate and simplify this model to simulate molten metal powder, several assumptions and considerations were not taken into account. By creating a simplified model, this establishes that the model is manageable and able to produce results that are of focus for this study. Some of the model assumptions and equations were derived from previous studies. This built model was later employed to verify previous studies as well as obtain new results for a selection of alloys. The objective of the model was to gain greater insight on the selection of utilizing optimal processing parameters and droplet behavior during the GA process. Influences that attributed to the velocity and thermal behavior of droplets consisted of the selection of the droplet diameter size, gas composition, atomization gas pressure and melt superheat temperature. Some of the assumptions of the model include spherical droplets were created, Newtonian cooling with forced convection and axial distance or one-dimensional travelling only. Assumptions include solely mean gas flow consideration and no phase transformation was accounted for. To substitute for this assumption of phase transformation, an energy balance or conservation equation was utilized. Through the application of creating the model and verifying previous studies, several conclusions were reached:

- It is worth noting that 1D modeling was capable of producing similar results from studies that assumed 2D travel. It is essentially illustrated that the complexity of utilizing 2D modeling for droplet travel may not be necessary in obtaining results
- Analysis and research illustrated that as the droplet diameter size increases, the velocity, droplet temperature change and cooling rate of the droplet decreases
- Smaller droplets are able to produce higher velocities due to their ability of not being able to resist the drag forces that cause acceleration and deceleration as opposed to larger droplets. This higher velocity translates to higher change of droplet temperature and higher values of cooling rate. A higher cooling rate is due to the fact that smaller droplets transfer heat at a quicker rate than larger ones
- In regards to this study and the alloys selected for research, Helium (He) is a far more superior atomization gas when compared to Argon (Ar). Helium is able to absorb the heat and facilitate the transfer of heat much quicker than the other two. This trait allows for the droplets to cool faster and produce more efficient results

Acknowledgment

This paper summarizes the findings of a research work funded by the National Nuclear Security Administration (NNSA). Any findings and recommendations expressed in this paper are those of the authors.

Funding Information

The work reported here was financially supported by the National Nuclear Security Administration (NNSA)

Author's Contributions

Genaro Pérez-de León: Participated in all modeling, data-analysis and contributed to the writing of the manuscript.

Vincent E. Lamberti: Participated in modeling, data-analysis and contributed to the writing of the manuscript.

Roland D. Seals: Participated in modeling plan, data-analysis and contributed to the writing of the manuscript.

Taher M. Abu-Lebdeh: Participated in modeling plan, data-analysis and contributed to the writing of the manuscript.

Sameer A. Hamoush: Participated in all modeling, data-analysis and contributed to the writing of the manuscript.

Ethics

Reference

AMT, 2014. Gas-atomization. Advanced Materials Technology.

Cai, W. and E.J. Lavernia, 1998a. Modeling of porosity during spray forming: Part I. Effects of processing parameters. Metallurgical Mater. Trans. B, 29: 1085-1096. DOI: 10.1007/s11663-998-0078-y

Cai, W. and E.J. Lavernia, 1998b. Modeling of porosity during spray forming: Part II. Effects of atomization gas chemistry and alloy compositions. Metallurgical Mater. Trans. B, 29: 1097-1106.

DOI: 10.1007/s11663-998-0079-x

Clemens, H. and W. Smarsly, 2011. Light-weight intermetallic titanium aluminides-status of research and development. Adv. Mater. Res., 278: 551-556. DOI: 10.4028/www.scientific.net/AMR.278.551

Dormand, J.R. and P.J. Prince, 1980. A family of embedded Runge-Kutta formulae. J. Comput. Applied Math., 6: 19-26. DOI: 10.1016/0771-050X(80)90013-3

EFMPCL., 2008. Gas atomisation iron melting refining furnace for processing metals alloys powders production line. Easy Fashion Metal Products Co. Ltd.

Giri, V.S., R. Sarathi, S. Chakravarthy and C. Venkataseshaiah, 2004. Studies on production and characterization of nano-Al_2O_3 powder using wire explosion technique. Mater. Lett., 58: 1047-1050. DOI: 10.1016/j.matlet.2003.08.015

Grant, P., 1995. Spray forming. Progress Mater. Sci., 39: 497-545. DOI: 10.1016/0079-6425(95)00004-6

Li, B., X. Liang, J. Earthman and E. Lavernia, 1996. Two dimensional modeling of momentum and thermal behavior during spray atomization of γ-TiAl. Acta Mater., 44: 2409-2420. DOI: 10.1016/1359-6454(95)00335-5

Shampine, L.F. and M.W. Reichelt, 1997. The MATLAB ODE suite. SIAM J. Scientific Comput., 18: 1-22. DOI: 10.1137/S1064827594276424

Shampine, L.F. and M.W. Reichelt, 1999. Solving Index-1 DAEs in MATLAB and simulink. SIAM Rev., 41: 538-552. DOI: 10.1137/S003614459933425X

Zheng, B., Y. Lin, Y. Zhou and E.J. Lavernia, 2009a. Gas atomization of amorphous aluminum: Part I. Thermal behavior calculations. Metallurgical Mater. Trans. B, 40: 768-778. DOI: 10.1007/s11663-009-9276-5

Zheng, B., Y. Lin, Y. Zhou and E. Lavernia, 2009b. Gas atomization of amorphous aluminum powder: Part II. Experimental investigation. Metallurgical Mater. Trans. B, 40: 995-1004. DOI: 10.1007/s11663-009-9277-4

Nomenclature

v_{g0} = initial velocity of atomization gas in m/s
M_a = Mach number at the nozzle exit
v_s = sonic velocity at the nozzle exit in m/s
C_M = correlation coefficient used to account for friction effects and the difference between the nozzle used an ideal convergent-divergent one
P_0 = atomization gas pressure in MPa
P_e = atomization gas pressure at the nozzle exit that approximates the chamber pressure in MPa
γ = ratio of constant pressure to constant volume specific heat
T_e= atomization gas temperature at the nozzle exit in K
m_{mol} = molar mass of the atomization gas in kg/mol
T_0 = atomization gas temperature at the stagnation point (i.e., atomization pressure) in K
v_g = axial gas velocity in m/s
z = flight distance in m
λ = gas velocity decay coefficient
ρ_d = density of droplet in kg/m³
V_d = volume of droplet in m³
$\left(\frac{dv_d}{dt}\right)$ = droplet motion or velocity with respect to time
ρ_g = density of the gas atomization gas in kg/m³
g = gravitational acceleration in m/s²
A_s = cross-sectional area of droplet in m²
C_d = spherical droplet during gas atomization drag coefficient
v_d = velocity of droplet in m/s
v_g = velocity of the gas atomization gas in m/s
Re = Reynolds number
d = droplet size diameter in m
μ_g = gas dynamic viscosity in (N*s)/m²
h = convective heat transfer coefficient between a droplet and the atomization gas in W/(m²*K)
fr = consideration of gas/melt flow ratio
A_d = droplet surface area in m²
T = droplet temperature in K
T_{gas} = temperature of the ambient atomization gas in K
ε = emissivity
σ = Stephan-Boltzmann constant
C_{pd} = specific heat capacity in Joules per mole-Kelvin (J/(mole*K))
K_g = thermal conductivity of gas in W/(m*K)
Pr = Prandtl number, unit-less
C_{pg} = gas specific heat in Joules per kilogram-Kelvin (J/(kg*K))
$\dot{T}$ = cooling rate of the droplets in K
T_{melt} = droplet/melt superheat temperature in K
T_{gas} = temperature of the ambient atomization gas in K
ρ_m = density of droplet/melt in kg/m³